SUPPORTING INFORMATION

Mixing Aβ(1-40) and Aβ(1-42) peptides generates unique amyloid fibrils

Linda Cerofolini[a], Enrico Ravera[a,b], Sara Bologna[a,b], Thomas Wiglenda[c], Annett Böddrich[c], Bettina Purfürst[d], Iryna Benilova[e,§], Magdalena Korsak[f,ǀ], Gianluca Gallo[a,b,#], Domenico Rizzo[a,b], Leonardo Gonnelli[a,b], Marco Fragai[a,b], Bart De Strooper*[,e,g], Erich E. Wanker*[,c], Claudio Luchinat*[,a,b,f]

a. Magnetic Resonance Center (CERM), University of Florence and Interuniversity Consortium for Magnetic Resonance of Metalloproteins (CIRMMP), Via L. Sacconi 6, 50019, Sesto Fiorentino (FI), Italy

b. Department of Chemistry "Ugo Schiff", University of Florence, Via della Lastruccia 3, 50019, Sesto Fiorentino (FI), Italy

c. Neuroproteomics, Max Delbrück Center for Molecular Medicine, Robert-Roessle-Strasse 10, 13125 Berlin, Germany

d. Core facility electron microscopy, Max-Delbrück Center for Molecular Medicine, Robert-Roessle-Strasse 10, 13125 Berlin, Germany

e. VIB Center for Brain and Disease research, Herestraat 49, 3000 Leuven, Belgium

f. Giotto Biotech S.R.L., Via Madonna del Piano 6, 50019 Sesto Fiorentino (FI), Italy.

g. KULeuven, Department of Neurology, Herestraat 49, 3000 Leuven, Belgium

[§]Current address: MRC Prion Unit at UCL, Institute of Prion diseases, Courtauld building, 33 Cleveland Street, London W1W7FF, UK.

[ǀ]Current address: Roche Polska Sp. zo. o. Domaniewska 28, 02-672 Warszawa, Poland.

[§§] Current address: Fresenius Kabi, Via Camagri 41, Verona, Italy.

* To whom correspondence may be addressed. Email: claudioluchinat@cerm.unifi.it, ewanker@mdc-berlin.de, bart.destrooper@cme.vib-kuleuven.be.

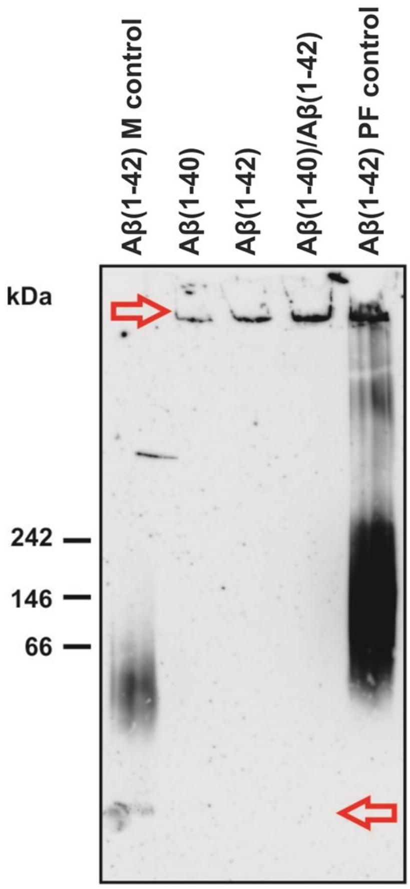

Figure S1. Native polyacrylamide gel electrophoresis of mature fibrils showing no sign of smaller aggregates; Arrows indicate high molecular weight aggregates (top) and monomers (bottom), respectively. The abbreviation PF stand for protofibrils, M for monomers. The prepared amyloid fibrils are detectable in the gel pockets, while monomers or smaller protofibrillar Aβ(1-42) oligomers, which were used as controls, can enter the separating gel. This indicates that all three aggregate preparations contain large, relatively stable structures that cannot be dissociated with native polyacrylamide gels.

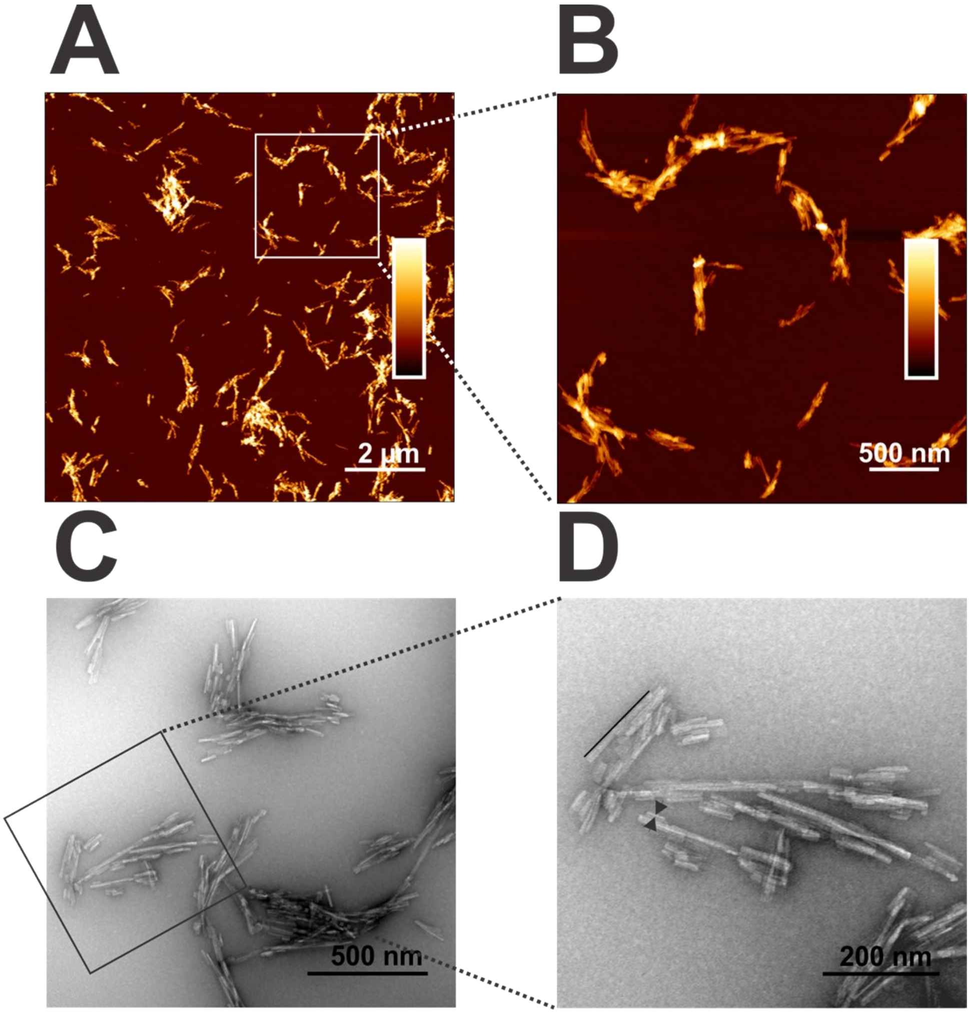

Figure S2. Analysis of 1:1 Aβ(1-42):Aβ(1-40) mixed fibrils by AFM (A, B) and TEM (C, D). B) and D) show a detail from A and C in higher magnification (see frames). A) and B) color gradient: 0-40 nm height. D) The line and the arrowheads illustrate how the length and breadth of fibrils were determined. Under the fibrillization conditions used in the present work the resulting fibrils appear short and highly associated in flat bundles, which do not disassemble to isolated fibrils upon sonication (data not shown). For length determination 592 fibrils have been measured which show an average length of 106.61 nm (SD = 54.75). For breadth determination 244 fibrils have been analyzed which show an average breadth of 3.25 nm (SD = 0.67).

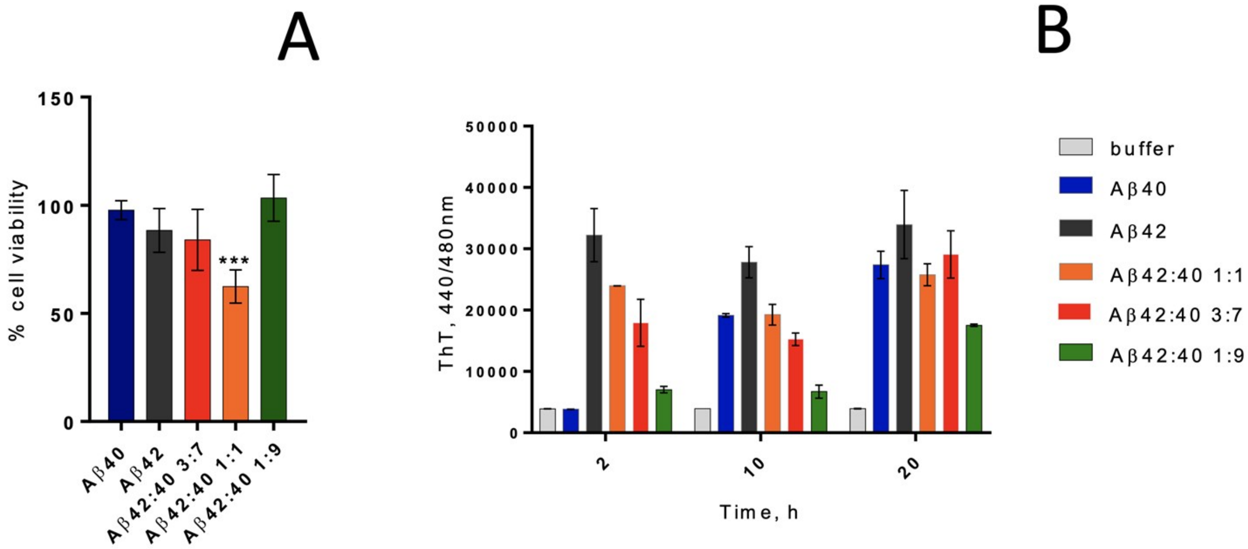

Figure S3. (A) Viability of primary hippocampal mouse neurons in a Cell-Titer blue assay after 72 h treatment with 10 μM of pre-aggregated pure Aβ(1-40), pure Aβ(1-42), and mixture of Aβ(1-42):Aβ(1-40) peptides in different ratios. In this assay only the 1:1 Aβ(1-42):Aβ(1-40) preparations induce a significant reduction of cell viability of about 30 % (Mean±St.Dev.,***$p<0.001$, 2-tailed unpaired t-test, comparison to untreated cells, n=3-4). All other preparations did not significantly reduce cell viability, indicating that they are less toxic than the 1:1 Aβ(1-42):Aβ(1-40) preparations. Note that non-aggregated and aggregated Aβ preparations at a concentration below 10 μM did not show any cytotoxicity under the same conditions. (B) Presence of fibrillar (Thioflavin-T reactive) species in the samples at different incubation times. Mean±St.Dev., ThT concentration 12 μM (*vide infra*).

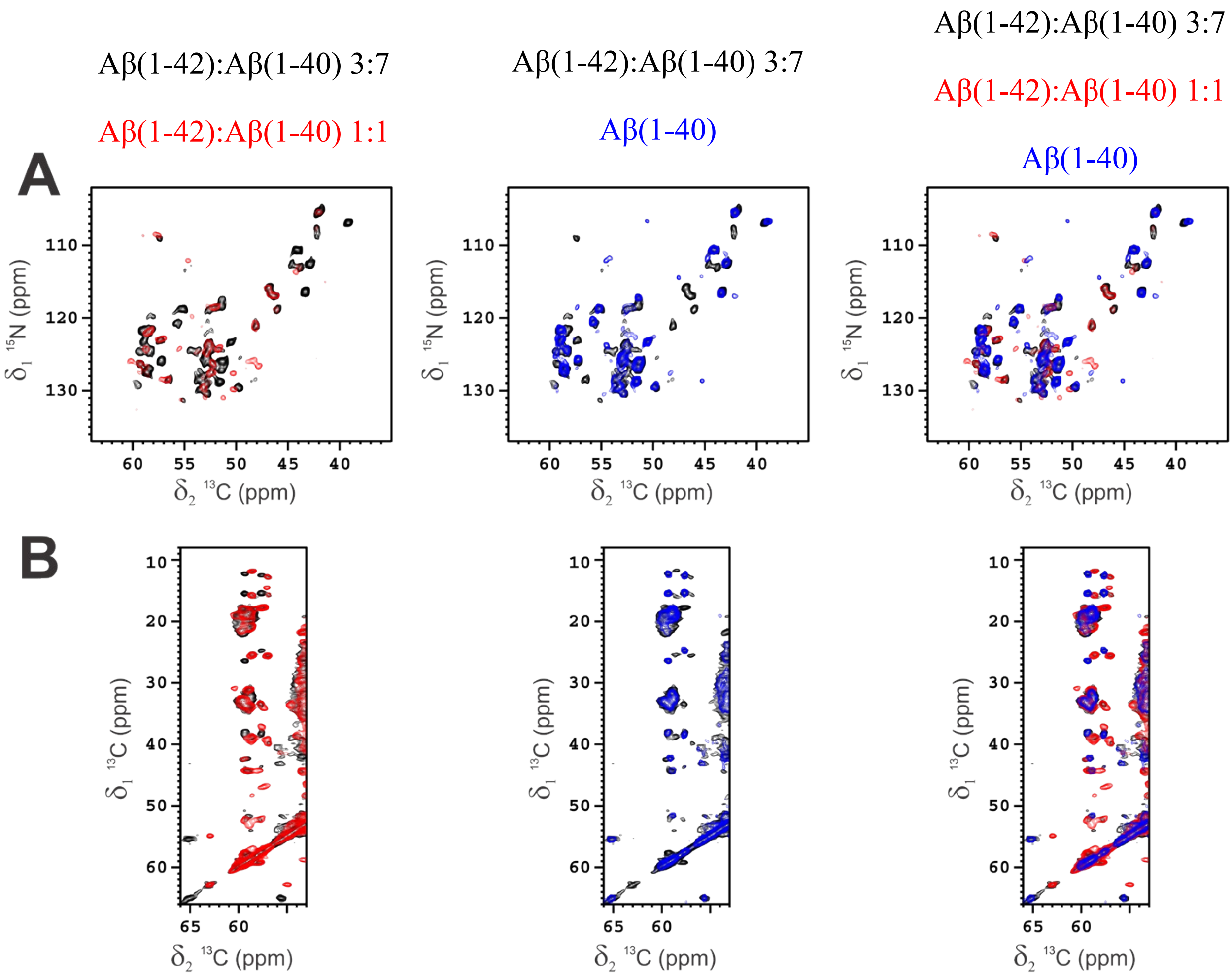

Figure S4. A) 2D ^{15}N-^{13}C NCA spectra of the Aβ(1-42):Aβ(1-40) mixed fibrils in the 3:7 molar ratio (black) overlaid with the 2D ^{15}N-^{13}C NCA spectra of Aβ(1-42):Aβ(1-40) mixed fibrils in the 1:1 molar ratio (red) and with fibrils of pure Aβ(1-40) (blue). Magnetic field: 700 MHz (16.4 T), dimension of rotor: 3.2 mm (~10-14 mg of fibrils), 14 kHz spinning, 100 kHz ^{1}H decoupling. B) 2D ^{13}C-^{13}C correlation spectra (in the region of the Cα of the isoleucine residues) of the Aβ(1-42):Aβ(1-40) mixed fibrils in the 3:7 molar ratio (black) overlaid with the 2D ^{13}C-^{13}C correlation spectrum of Aβ(1-42):Aβ(1-40) mixed fibrils in the 1:1 molar ratio (red) and with 2D ^{13}C-^{13}C-correlation spectrum of fibrils of pure Aβ(1-40) (blue). Magnetic field: 700 MHz (16.4 T), dimension of rotor: 3.2 mm (~10-14 mg of fibrils), 12 kHz spinning, 100 kHz ^{1}H decoupling.

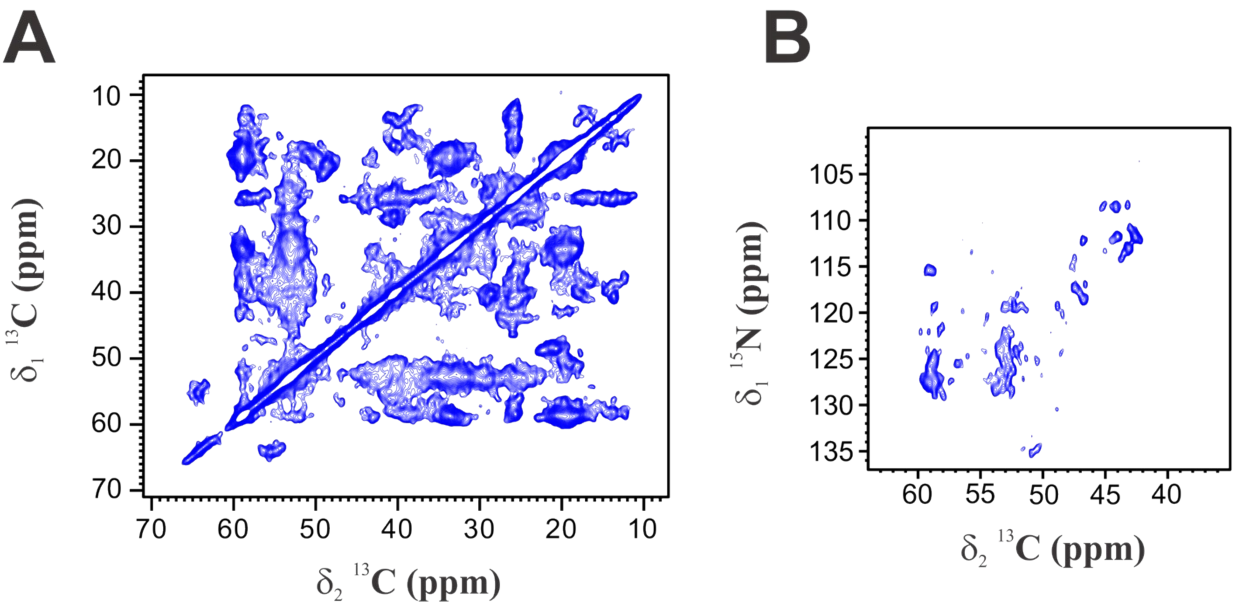

Figure S5. A) 2D ^{13}C-^{13}C correlation spectrum of the Aβ(1-42) aggregates. Magnetic field: 700 MHz (16.4 T), dimension of rotor: 3.2 mm (~10-14 mg of aggregates), 12 kHz spinning, 100 kHz ^{1}H decoupling; B) 2D ^{15}N-^{13}C NCA spectrum of the Aβ(1-42). Magnetic field: 700 MHz (16.4 T), dimension of rotor: 3.2 mm (~10-14 mg of aggregates), 14 kHz spinning, 100 kHz ^{1}H decoupling.

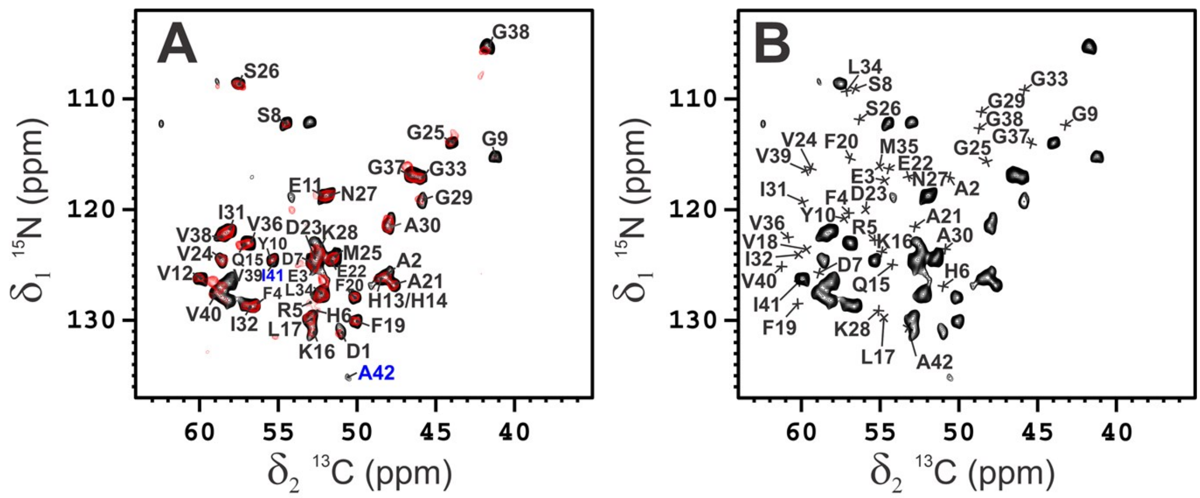

Figure S6. (A) 2D ^{15}N-^{13}C NCA spectrum of the Aβ(1-42) component (black) overlaid with the 2D ^{15}N-^{13}C NCA spectrum of the Aβ(1-40) component (red) in the 1:1 Aβ(1-42):Aβ(1-40) mixed fibrils; the full assignment of the spectrum is shown. (B) 2D ^{15}N-^{13}C NCA spectrum of the Aβ(1-42) component (black), with the assignments of the S-shaped fibrils [1].

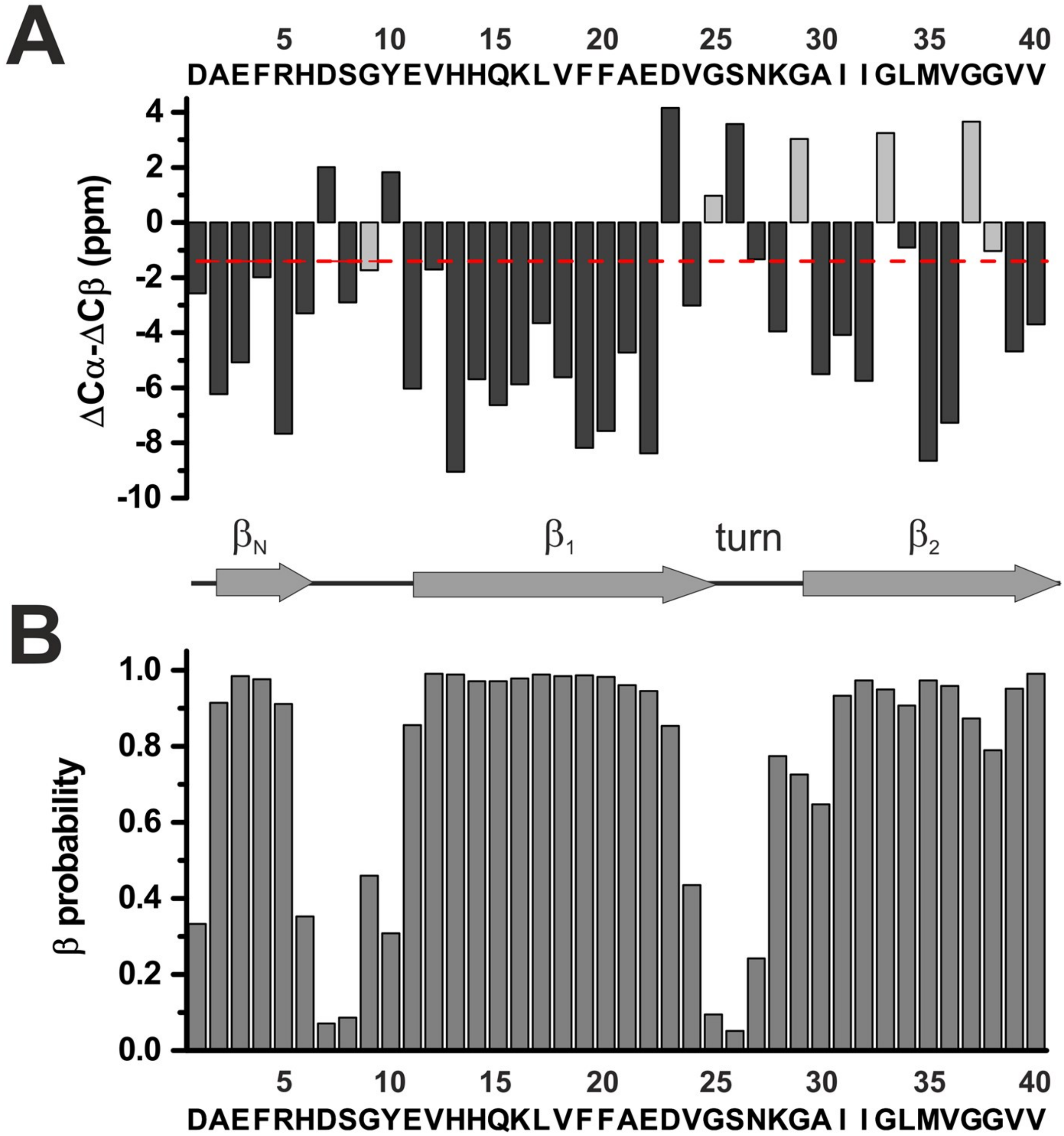

Figure S7. Secondary structural analysis of Aβ(1-42):Aβ(1-40) mixed fibrils (1:1 ratio). Chemical shift differences with respect to the corresponding random coil values (panel A) and residue specific β-probabilities predicted by TALOS+ (panel B) are displayed. In panel A the red line indicates the cutoff of -1.4 ppm and the ΔδCα shifts for the glycines are displayed in light-grey.

Table S1. Long-range intramolecular contacts between β_1- and β_2-strands observed and used for deriving the structural models of Aβ(1-42):Aβ(1-40) mixed fibrils in the present work.

Number	Contacts	Source spectra
1	H13 Cε_1 - V40 Cβ	DARR (300 ms)
2	H13 Cγ - V40 Cγ_2	DARR (300 ms)
3	H13 Cγ - V40 Cβ	DARR (300 ms)
4	L17 Cβ - L34 Cδ_2	DARR (100 ms)
5	L17 Cβ - L34 Cδ_1	DARR (100 ms)
6	L17 Cβ - L34 Cβ	DARR (100 ms)
7	L17 Cδ_1 - V36 Cγ_1	DARR (100 ms)
8	L17 N - L34 Cδ_2	PAIN(10ms)
9	L17 N - L34 Cδ_1	PAIN(10 ms)
10	F19 Cδ_1 - L34 Cδ_2	DARR (200 ms)
11	F19 Cβ - G33 Cα	DARR (100 ms)
12	A21 Cα - I32 Cγ_2	DARR (300 ms)
13	A21 Cβ - I32 Cγ_1	DARR (100 ms)
14	A21 Cβ - I32 Cβ	DARR (300 ms)
15	D23 Cβ - A30 Cβ	DARR (100 ms)

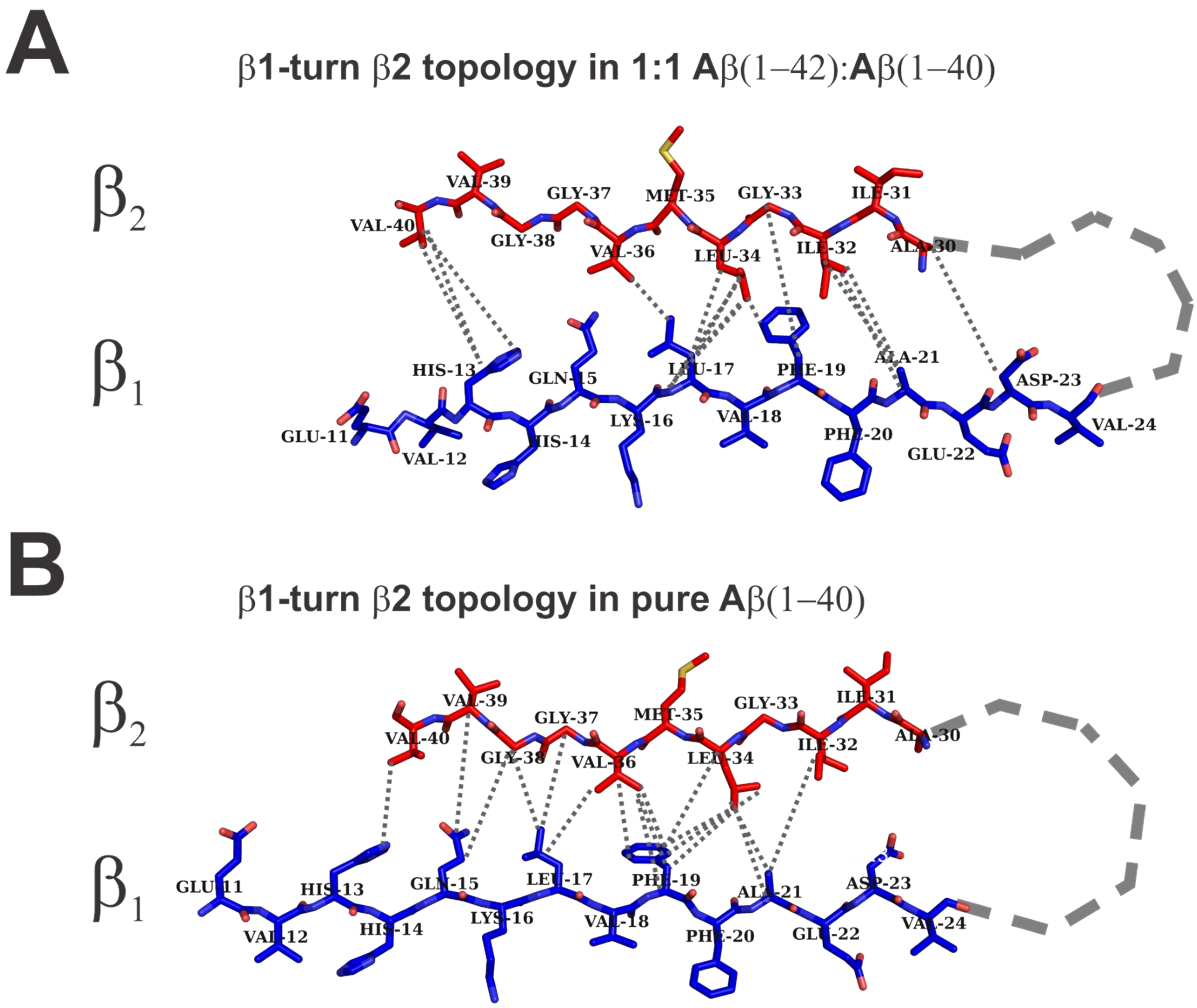

Figure S8. Folding of the monomeric Aβ(1-40) peptide in the model of 1:1 Aβ(1-42):Aβ(1-40) mixed fibrils (A) and in the model obtained for the fibrils of pure Aβ(1-40) [2] (B). It is clear that, in the current conformation of the β–arch, the contacts indicate a reciprocal packing of the two β-strands (β_1 and β_2) (A), which is different from that previously calculated for the fibrils of pure Aβ(1-40) [2] (B), but is consistent with the contacts observed in reference [10].

Table S2. Long-range intermolecular contacts between two β_2-strands observed and used for deriving the structural models of Aβ(1-42):Aβ(1-40) mixed fibrils in present work. The contacts of the side chains of Ile31 with Gly38/Val39/Val40, and of Met35 with Gly38/Val39, indicate the presence of a head-to-tail antiparallel association of two β_2-strands of different monomers. These experimental restraints are in agreement with a two-fold rotational symmetry (also reported for the co-aligned homo-zipper model [3]) and with the parallel registry of the protofilament.

Number	Contacts	Source spectra
1	M35 Cε - V39 Cβ	DARR (200 ms)
2	M35 Cβ - G38 Cα	PDSD (400 ms)
3	I31 $C\delta_1$ - G38 Cα	PDSD (400 ms)
4	I31 $C\gamma_2$ - G38 Cα	PDSD (400 ms)
5	I31 Cβ - V39 $C\gamma_1$	DARR (200 ms)
6	I31 $C\delta_1$ - V39 $C\gamma_2$	DARR (200 ms)
7	I31 $C\gamma_2$ - V39 C	DARR (100 ms)
8	I31 $C\gamma_2$ - V39 Cβ	DARR (200 ms)
9	I31 $C\gamma_2$ - V39 $C\gamma_2$	DARR (100 ms)
10	I31 $C\gamma_2$ - V40 $C\gamma_1$	DARR (200 ms)

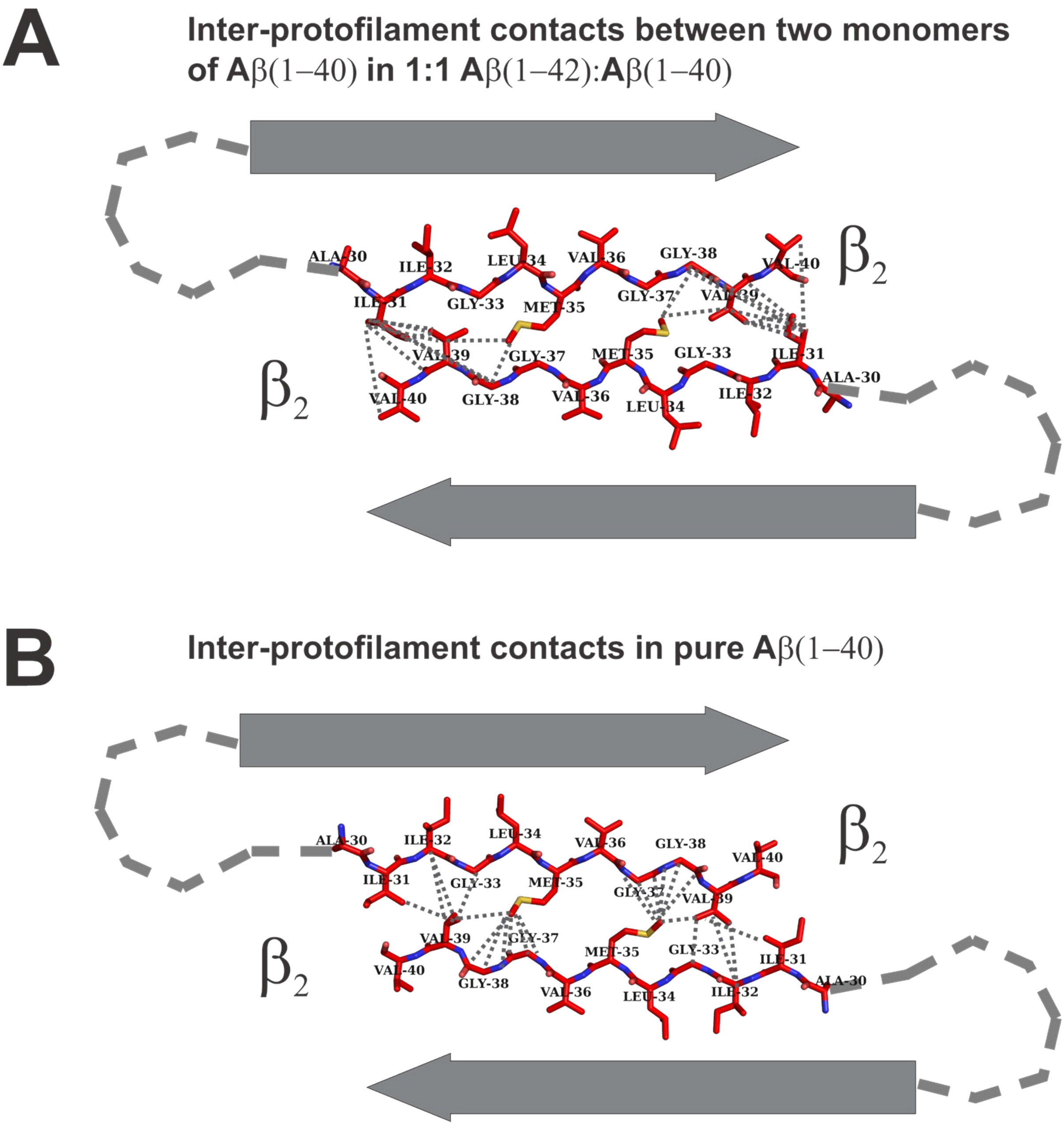

Figure S9. Lateral packing of two different protofilaments in the model of 1:1 Aβ(1-42):Aβ(1-40) mixed fibrils (A) and in the model of the fibrils of pure Aβ(1-40) [2] (B), calculated implementing long-range distance restraints in HADDOCK [4]. The contacts and the generated model (A) are similar, but not identical, to those of the pure Aβ(1-40) (B) [2]. In particular, the contacts Ile32-Val39, Gly33-Val39 and Met35-Gly37 are not observed in the mixed fibrils, while the additional contact between Ile31 and Val40 is observed because of the higher rigidity of Val40.

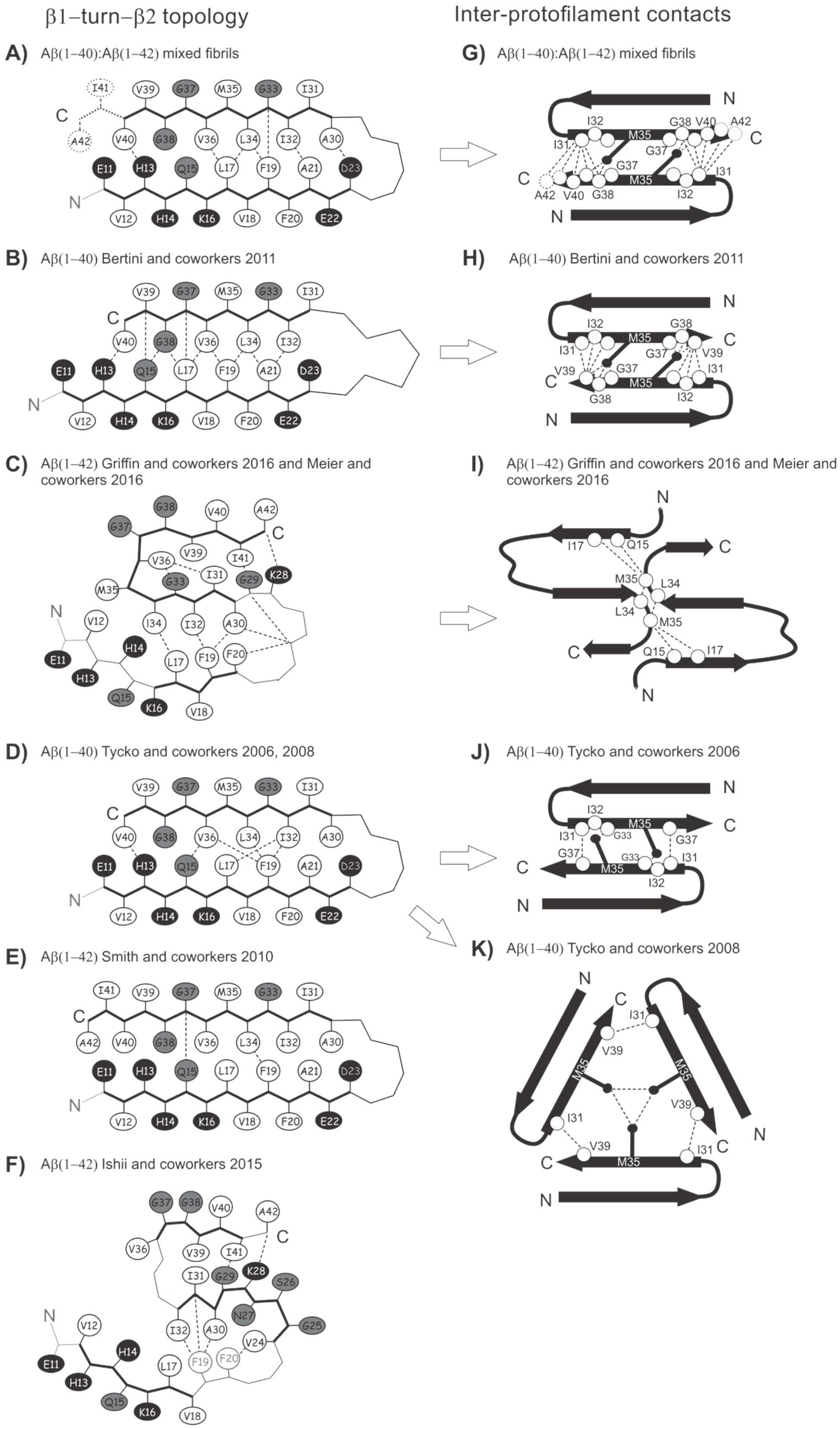

Scheme S1. Different β-strand zippers in various SS-NMR-derived structural models of Aβ fibrils. The topologies of the β_1-turn-β_2 motif identified in the present work (A) and in other previously studied Aβ(1-40) fibrils (B, D) [2,5–7] and Aβ(1-42) fibrils (C, E, F) [8–10] are shown in the left column. The dashed/dotted lines represent unambiguous experimental restraints used to derive the corresponding topology. In the schematic description of distinct structures of the U-shaped motif, the hydrophobic, acidic/basic, and other types of residues are shown in white, black, and gray, respectively. The topologies of the interprotofilament interface (β_2-β_2 zippers) in the fibrils determined in the present work (G) and proposed in previous studies (H, I, J, K) [2,5,6] are shown in the right column. The dashed lines represent unambiguous experimental restraints used to derive the corresponding topology. The filled black circles represent the Cε of the Met35 residue. Other residues included in SS-NMR-observed structural restraints for linking the two β_2-strands are shown as hollow circles. Residues Ile41 and Ala42, in the present model of the mixed fibrils, are indicated with dashed circles to stress that both Aβ(1-40) and Aβ(1-42) share the same arrangement.

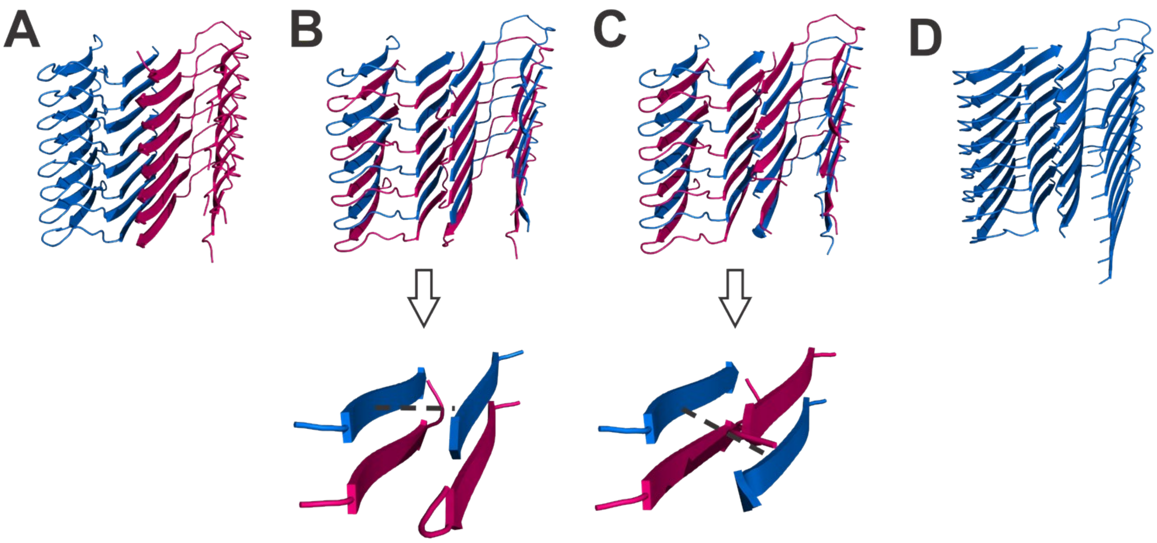

Figure S10. Possible reciprocal packing modes of Aβ(1-40) and Aβ(1-42) peptides along the fibril axis generated and scored by HADDOCK 2.2 [4]: homogeneous protofilaments (all composed of either Aβ(1-40) or Aβ(1-42) peptides) that form a mixed cross-β structure (model A); interlaced protofilaments that form a paired (model B), or staggered (model C) cross-β structure. The Aβ(1-42) polypeptide is colored magenta and the Aβ(1-40) polypeptide in blue. The model of pure Aβ(1-40) fibrils is also displayed (panel D).[2] Model A is excluded by the presence of cross-peaks between the N-terminus and C-terminus of the β_2 strand. Arrangements B and C are very similar and equally possible (see Table S3).

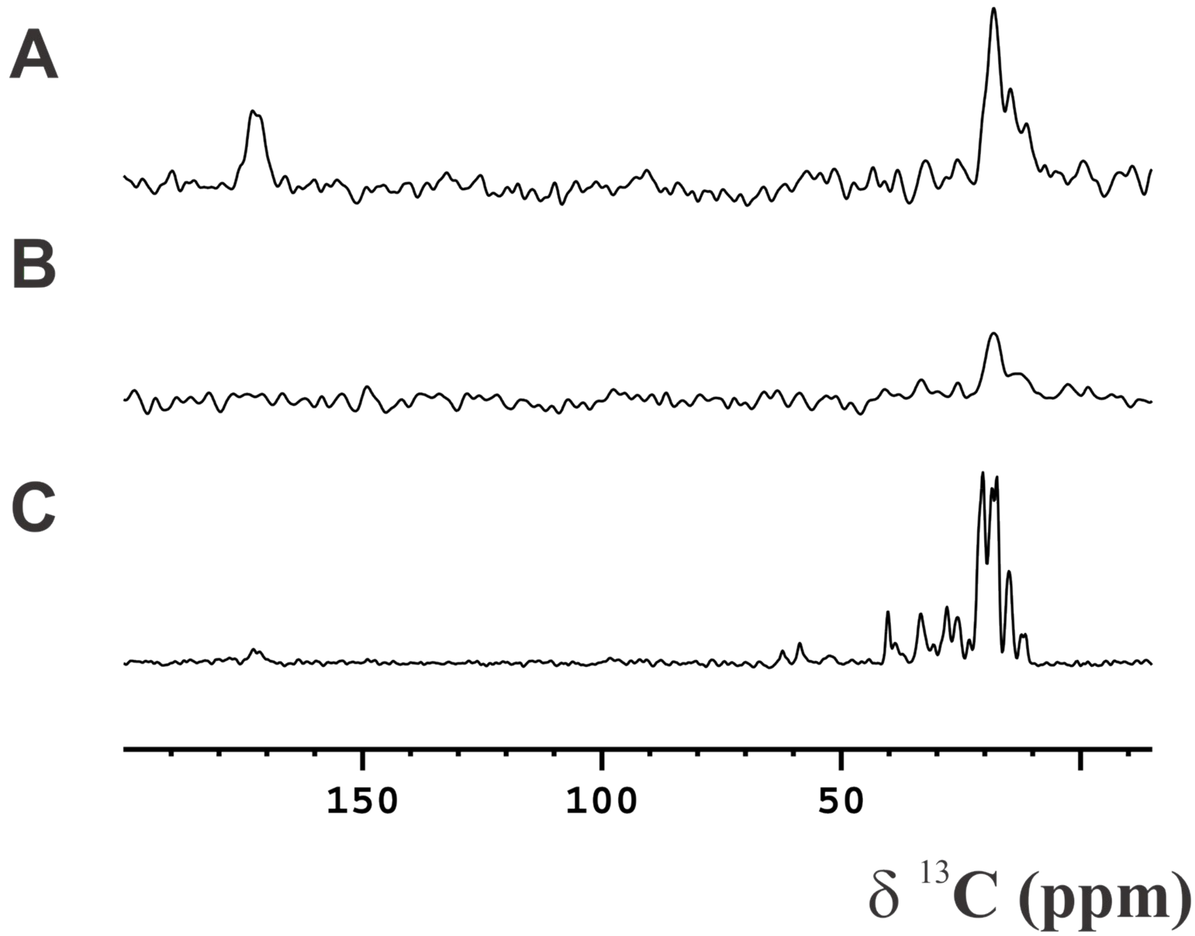

Figure S11. 1D zTEDOR spectra of the Aβ(1-42):Aβ(1-40) mixed fibrils in the 1:1 molar ratio, where A) Aβ(1-42) is ^{15}N-enriched and Aβ(1-40) is ^{13}C-enriched and B) Aβ(1-42) is ^{15}N-enriched and Aβ(1-40) is in natural abundance, and C) Aβ(1-42) is in natural abundance and Aβ(1-40) is ^{15}N-^{13}C-enriched. Magnetic field: 800 MHz (19 T, 201.2 MHz ^{13}C Larmor frequency), dimension of rotor: 3.2 mm, 16 kHz spinning, 80 kHz ^{1}H decoupling. The number of scans was tuned according to the sample amount (10240, for sample A and C, and 40960 for sample B). The signal of the backbone carbonyls appears only in (A), whereas it is absent in (B), confirming an interlaced arrangement. The spectrum (C) shows relatively lower intensity in the carbonyl region because the coupling across the hydrogen bond is masked by other intra-filament couplings.

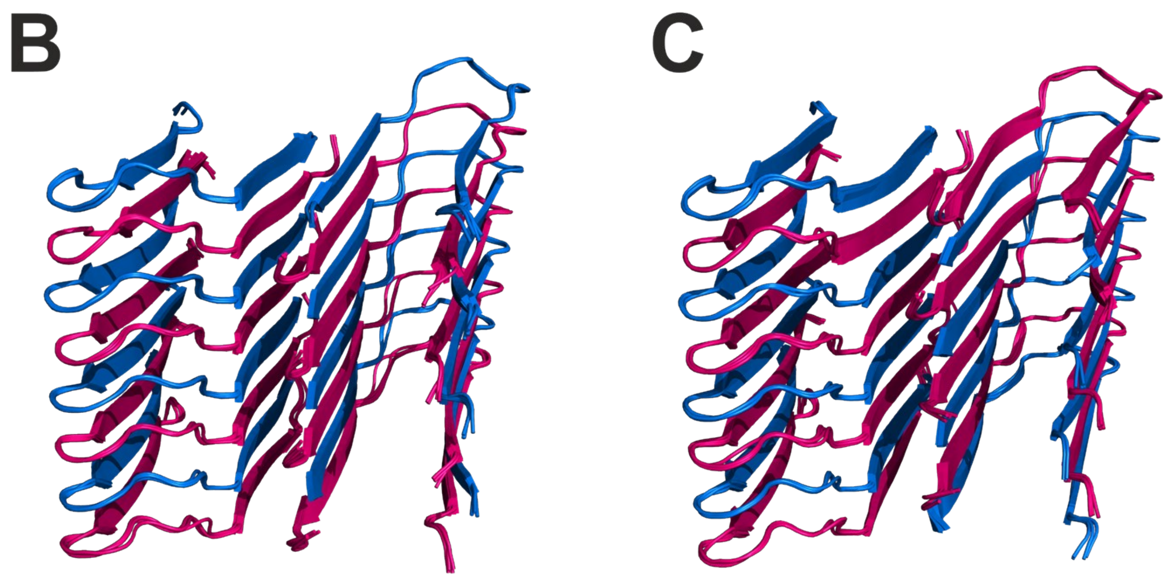

Figure S12. Family of the best four structures corresponding to model B (left) and model C (right), obtained with an experimental restraint-driven calculation with HADDOCK 2.2. Two identical interlaced Aβ(1-40)/Aβ(1-42) protofilaments (left) and two different interlaced protofilaments, Aβ(1-40)/Aβ(1-42) and Aβ(1-42)/Aβ(1-40) (right) have been considered, respectively, in the calculations. The HADDOCK-scores for the models of the two families are not very different, although somewhat more favorable for the right-hand model (Table S3), so that firm conclusions for one or the other model cannot be drawn.

Table S3. HADDOCK statistics evaluated on the 200 water refined models. The reported data are related to the best four structures of the clusters with the lowest HADDOCK-scores. The packing density and number of cavities have been evaluated using the Voronoia plugin in Pymol [11].

	Model B	**Model C**
HADDOCK-Score	-353 ± 5	-267 ± 2
HADDOCK-Score (without E_{AIR})	-394 ± 5	-299 ± 2
N° of structures of the cluster	199	200
RMSD	0.3 ± 0.2	0.3 ± 0.2
Desolvation Energy	-185 ± 4	-150 ± 5
Buried surface area (BSA)	4862 ± 33	4686 ± 21
Ambiguous interaction restraint energy (E_{AIR})	418 ± 23	321 ± 8
Average packing density	0.81 ± 0.01	0.82 ± 0.01
Number of cavities	22 ± 4	29 ± 5

Table S4. HADDOCK statistics evaluated on the water refined models of model B, fibrils of pure Aβ(1-40) and fibrils of pure Aβ(1-42) in the S-shaped conformation after HADDOCK minimization. The reported data are related to the best four structures of the clusters with the lowest HADDOCK-scores.

	Model B	**Aβ(1-40)** [2]	**Aβ(1-42)** [12] **S-shaped conformation**
HADDOCK-Score	-353 ± 5	-322 ± 3	-407 ± 0.4
HADDOCK-Score (without E_{AIR})	-394 ± 5	-326 ± 3	-408 ± 0.4
RMSD	0.3 ± 0.2	0.2 ± 0.1	0.2 ± 0.1
Desolvation Energy	-185 ± 4	-135 ± 4	-104 ± 5
Buried surface area (BSA)	4862 ± 33	4073 ± 30	5617 ± 71
Ambiguous interaction restraint energy (E_{AIR})	418 ± 23	38 ± 4	15 ± 2

Table S5. HADDOCK statistics evaluated on 20 water refined models. The reported data are related to the best four structures. The calculations were performed on the HADDOCK2.2 web-server using the *refinement* interface. The models that were refined derived from calculations where the last residues of Aβ(1-42) were left free without the imposition of β-strand restraints.

	Aβ(1-40) monomer conformation of Bertini et al. 2011	**Aβ(1-40) monomer conformation of current work**	**Aβ(1-42) monomer conformation of Bertini et al. 2011**	**Aβ(1-42) monomer conformation of current work**	**Aβ(1-40)/ Aβ(1-42) monomer conformation of current work**
HADDOCK-Score	-238 ± 3	-205 ± 2	-204 ± 3	-235 ± 3	-266 ± 1
N° of structures of the cluster	20	20	20	20	20
RMSD	0.3 ± 0.2	0.3 ± 0.2	0.3 ± 0.2	0.3 ± 0.2	0.3 ± 0.2
Desolvation Energy	-57 ± 1	-37 ± 1	-49 ± 6	-68 ± 5	-58 ± 1
Buried surface area (BSA)	4072 ± 29	3979 ± 22	4703 ± 56	4661 ± 40	4888 ± 37
Ambiguous interaction restraint energy (E_{AIR})	7 ± 2	19 ± 2	7 ± 2	18 ± 4	21 ± 1

Methods

Expression, purification, and sample preparation of Aβ(1-42):Aβ(1-40) mixed fibrils

The cDNAs encoding the Aβ(1-40) and Aβ(1-42) polypeptides were cloned in the pET3a vector using the NdeI and BamHI restriction enzymes. The peptides were expressed in the BL21 (DE3)pLys *E. coli* strain.

The peptides were purified as reported in the literature [2,13–16] with the modification of using a combination of anion-exchange and size exclusion chromatography. All the manipulations were performed at slightly alkaline pH in order to avoid the formation of structural contaminants produced by isoelectric precipitation. The inclusion bodies were first solubilized with 8 M urea and then purified by ion exchange chromatography performed in batch. All the obtained fractions of the diluted proteins were concentrated to a final volume using an Amicon device. The next step of purification was gel filtration, which was performed using the preparative column Sephadex 75 HiLoad 26/60 with 50 mM $(NH_4)OAc$ pH 8.5 as a buffer. The obtained fractions were collected together and concentrated. During all the purification steps, the protein purity was analysed by SDS-PAGE, whereas the protein concentration was estimated spectrophotometrically.

Both Aβ(1-42) and Aβ(1-40) bear the exogenous N-terminal Met0 due to the introduction of a translation start codon that has been shown previously to not significantly influence aggregation or toxicity of Aβ aggregates [16,17]. Both peptides were expressed using the Marley method [18], and purified as reported in literature [2,13–16] but using a combination of anion-exchange and size exclusion chromatography [2]. These two-steps of purification allowed us to obtain highly pure products with the yield in the range of 10 mg for Aβ(1-40) and 5-10 mg for Aβ(1-42) per liter of culture [19–21].

The fibrils for SS-NMR studies were produced as described by Bertini et al. [2]. Some samples were obtained by mixing ^{13}C, ^{15}N-uniformly enriched Aβ(1-40) polypeptide with Aβ(1-42) in natural isotopic abundance. Solutions containing Aβ(1-42) and Aβ(1-40) (total concentration of 100 µM) in 50 mM ammonium acetate (pH 8.5) were incubated at 310 K under agitation (950 rpm) for 5 weeks. The 3:7 mixture sample was prepared using 30 µM and 70 µM of Aβ(1-42) and Aβ(1-40) respectively, while the 1:1 sample was produced using the same concentration (50 µM) of both proteins. The 3:7 sample spontaneously resulted in two species (see main text), one of which corresponds to the previously characterized pure Aβ(1-40), and the other is a different species. Assuming that all the available Aβ(1-42) 30 µM formed fibrils with a stoichiometric amount of Aβ(1-40), 40 µM of Aβ(1-40) are free to form pure fibrils that, having a symmetric dimer as basic unit, contribute to 4/3 times the signal intensity of the other species, in line with the experimental observation. Fibrils were collected by ultracentrifugation at 60,000 rpm and 277 K for 24 h. The pellet was washed with fresh and cold ultrapure water (Millipore) for three times (1 mL per time). About 14 mg of wet material were packed into a 3.2 mm ZrO_2 magic angle spinning (MAS) rotor at 277 K using an ultracentrifugal device (GiottoBiotech) [22,23]. The fibril samples were kept fully hydrated during all steps.

An equimolar mixture of ^{13}C, ^{15}N-uniformly enriched Aβ(1-42) polypeptide (50 μM) and Aβ(1:40) polypeptide (50 μM) in natural isotopic abundance was prepared using the same protocol.

^{13}C, ^{15}N-uniformly enriched Aβ(1-42) fibrils were also grown, incubating the Aβ(1-42) polypeptide at the concentration of 20 μM to slow down the oligomerization process.

Equimolar mixtures of Aβ(1-42) and Aβ(1-40) polypeptides with different labeling schemes [^{15}N-uniformly enriched Aβ(1-42)/^{13}C-uniformly enriched Aβ(1-40) and ^{15}N-uniformly enriched Aβ(1-42)/natural isotopic abundance Aβ(1-40)] were also prepared following the same protocol.

Preparation of Aβ(1-42) monomer solutions and Aβ(1-42) protofibrillar aggregates

Synthetic Aβ(1-42) peptide produced by Bachem (Bubendorf, Schwitzerland) was dissolved in 1,1,1,3,3,3-Hexafluoro-2-propanol (HFIP) for three days, aliquoted and then lyophilized. Monomeric Aβ(1-42) solutions were prepared by dissolving peptides in 10 mM NaOH, sonication for 5 min and dilution to the final concentration in low salt buffer (LSB, 1.9 mM KH_2PO_4, 8.1 mM K_2HPO_4, 10 mM NaCl, pH 7.4). Synthetic Aβ(1-42) peptide produced by the laboratory of Dr. Volkmar-Engert (Institute for Medical Immunology, Charité, Berlin, Germany) was dissolved in HFIP overnight, sonicated for 30 min, aliquoted and then lyophilized. HFIP-treated peptide was dissolved in 100 mM NaOH, sonicated for 5 min and diluted in LSB to a final concentration of 200 μM. The solution was incubated for 6 h in an Eppendorf Thermomixer (Wesseling-Berzdorf, Germany) at 310 K and 300 rpm. The protofibrillar aggregate species was aliquoted and stored at 193 K.

Separation of Aβ(1-42) aggregates by native gels.

Aβ aggregates or monomers (4.5 μL, 10 μM) were diluted with NativePAGE 4x sample buffer (2.5 μL, Invitogen/Thermo Scientific, Dreieich, Germany) and LSB. Samples were loaded onto a Novex Bis-Tris 4-16% gel (Invitogen/Thermo Scientific, Dreieich, Germany) and separated. Aggregates were transferred to a nitrocellulose membrane (GE Healthcare, Freiburg, Germany) and visualized using the 6E10 antibody (BioLegend, San Diego, US) and a mouse anti-POD detection antibody (Sigma, Taufkirchen, Germany). Secondary antibody binding was detected by chemiluminescence using ChemiGlow West Substrate (Alpha Innotech, Kasendorf, Germany); luminescence was measured using a FujiFilm LAS-3000 imager (Fuji, Kleve, Germany).

Microscopic characterization

For the AFM measurements of Aβ(1-42):Aβ(1-40) mixed fibrils, sheet mica (Glimmer V3; Plano, Wetzlar, Germany) was glued to a microscope slide and samples (20 µL) were adsorbed for 10 min onto the freshly cleaved mica, washed with freshly filtered deionized water (4×30 µL) and dried overnight. Dry AFM images were recorded on a Nanowizard II/Zeiss Axiovert setup (JPK, Germany) using intermittent contact mode and PPP-NCHAuD probes (NANOSENSORS™, Neuchâtel, Switzerland).

For the TEM measurement, samples of Aβ(1-42):Aβ(1-40) mixed fibrils were adsorbed onto formvar-carbon coated grids, stained with 5 % of uranyl acetate, and analyzed with a Morgagni electron microscope (Thermo Fisher), and a Morada camera. Pictures were taken and analyzed with the iTEM software (EMSIS GmbH, Münster, Germany).

Cell viability assay

Primary hippocampal neurons were prepared from trypsinized brains of 17-days old C57/Bl6 mouse embryos, and plated out in minimal essential medium (Invitrogen, catalogue no. 31095-029) supplemented with horse serum, penicillin, and streptomycin (PenStrep, Invitrogen, catalogue no. 15140-122). 4 h after plating, medium was replaced with Neurobasal medium (NB, Invitrogen, catalogue no. 21103-049) supplemented with B27 (Invitrogen, catalogue no. 17504-044), and PenStrep. Neurons were grown in B27-supplemented Neurobasal medium for 10 days, and then were treated with 10 µM of pre-aggregated Aβ(1-40), Aβ(1-42) and a mixture thereof (Fig. S3 A). Pre-aggregation was obtained from recombinant monomers incubated at the concentration of 100 µM in Tris-EDTA buffer (50 mM Tris, 1 mM EDTA, pH 7.4) for 2 h at room temperature. At this stage, Aβ(1-42) and preparations Aβ(1-42):Aβ(1-40) 1:1 and 3:7 demonstrated a pronounced Thioflavin T (ThT) incorporation whilst Aβ(1-40) and Aβ(1-42):Aβ(1-40) 1:9 still had a very low content of aggregates (Figure S3 B). Aβ(1-40) aggregation was detectable at 10 h and 20 h of incubation, and aggregation of Aβ(1-42):Aβ(1-40) 1:9 increased at 20 h of incubation (Figure S3 B). After 72 h treatment, 10 µL Cell-Titer-Blue dye (Promega) was added to 200 µL of the culture medium on the cells. After 3 h, the fluorescence intensity of the samples was measured at an excitation wavelength of 560 nm and an emission wavelength of 590 nm. Data was normalized to untreated cells (100%) and presented as Mean±St.Dev.; statistical significance is indicated by *** (Figure S3 A), $p<0.001$, 2-tailed unpaired t-test (comparison to untreated cells), n=3-4.

NMR measurements

^{15}N-^{13}C NCA and NCO (2D), NCACX, NCOCX, NCACB, N(CO)CACB and CANCO (3D) experiments were performed either on a Bruker Avance III 850 MHz wide-bore spectrometer (20.0 T, 213.7 MHz ^{13}C Larmor frequency), or on a Bruker Avance II 700 MHz wide-bore spectrometer (16.4 T, 176.1 MHz ^{13}C Larmor frequency) using 3.2 mm DVT MAS probeheads in triple-resonance mode. MAS frequency ($\omega_r/2\pi$) was set to 17.0, 14.0 or 12.0 kHz (± 2 Hz) depending on the experiment. The NCA, NCO, NCACX, NCOCX, NCACB, N(CO)CACB and CANCO experiments were carried out using the pulse sequences reported in the literature [24,25]. At 700 MHz NC transfers were achieved by optimal-control derived pulses [26]. Backwards CN transfer was achieved with a time-reversal of the same optimal-control pulses. The amount of material used to fill the rotor was ~ 10-14 mg; NCA and NCO experiments were acquired using 256 and 128 scans, respectively, with an acquisition time on t1 dimension of 9 ms, and a recycle delay of 1.8 sec; NCACX and NCOCX experiments were acquired using 64 and 32 scans, respectively, with an acquisition time of 7 ms on t1 dimension and of 6 ms on t2 dimension, and a recycle delay of 1.9 sec; NCACB and N(CO)CACB experiments were acquired using 64 and 144 scans, respectively, with an acquisition time of 5 ms on t1 dimension and of 4 ms on t2 dimension, and a recycle delay of 1.9 sec; CANCO experiment was acquired using 64 scans, with acquisition time of 5 ms on t1 dimension and of 6 ms on t2 dimension, and recycle delay of 2 sec.

2D ^{13}C-^{13}C proton-driven spin diffusion (PDSD) [27], dipolar-assisted rotational resonance (DARR) [27,28] and Second-order Hamiltonian among Analogous Nuclei Generated by Hetero-nuclear Assistance Irradiation (SHANGHAI) [29] correlation spectra with different mixing times (15 to 800 ms) were recorded on the 700 MHz instrument. For these experiments, the MAS frequency was stabilized at 12 kHz (± 2 Hz). SHANGHAI was included, with respect to the characterization reported in [2], because it warrants a more homogeneous transfer throughout signals at different frequencies at high field and moderate spinning rates. The ^{13}C-^{13}C correlation spectra were acquired using increasing number of scans with increasing mixing time (from 32 scans for shorter mixing times up to 96 scans for longer mixing times). For the sample of the 1:1 mixture of Aβ(1-42): Aβ(1-40) were Aβ(1-42) is ^{13}C-^{15}N isotopically enriched higher number of scans were employed since the amount of material was smaller (~8-10 mg; number of scan from 128 to 256). The acquisition time on t1 dimension was 8 ms and the recycle delay 1.9 sec.

Bidimensional (2D ^{15}N-^{13}C hNhhC, 500 μs HH mixing time) and monodimensional (zTEDOR, 10 ms mixing time) nitrogen and carbon correlation spectra were recorded on a Bruker AvanceIII spectrometer operating at 800 MHz (19 T, 201.2 MHz ^{13}C Larmor frequency) equipped with Bruker 3.2 mm Efree NCH probe-head. The spectra were recorded at 16 kHz (± 2 Hz) MAS frequency; the number of scans was 2048 for the bidimensional (10 ms of acquisition time on t1 dimension) and 10240 or 40960 (according to the fibril amount) for the monodimensional experiments, respectively; the recycle delay was 3 sec.

In all cases, ^{1}H decoupling was applied at 80-100 kHz (optimized on the basis of the $^{13}C'$ echo lifetime [30]) using sw$_f$TPPM [31–33]. During the experiments, the sample was cooled by a dry, cold air flow (> 935 L/h), and the effective sample temperature was estimated to be ~283 K [23].

Spectra were analyzed by the program CARA (Computer Aided Resonance Assignment, ETH Zurich) [34].

SS-NMR data analysis and structural modeling.

Sequential assignment of the new species present in the Aβ(1-42):Aβ(1-40) mixed fibrils, where either Aβ(1-40) or Aβ(1-42) was ^{13}C, ^{15}N-uniformly enriched, was performed using the same procedure for both samples, starting from the identification of the residues 31Ile-32Ile. These two consecutive residues can be identified following the signals of the two sidechains, which can be easily distinguished in the 2D ^{13}C-^{13}C correlation spectra. Starting from these residues, the sequential assignment was obtained by analyzing the 3D ^{15}N-^{13}C spectra according to the procedure reported by Bertini et al. [2]. The assignment is deposited in the BMRB with ID 34455). The secondary structure was predicted by TALOS+ [35] using the chemical shifts of the N, C, Cα and Cβ.

For model building, the length of the β_1 and β_2 strands was based on the secondary structure predicted by TALOS+. The β_1- and β_2-strands were then docked to one another by HADDOCK [4] using all the experimental long-range β_1-β_2 restraints. HADDOCK calculations were performed on the WeNMR GRID (http://www.wenmr.eu/, Guru interface, see supporting information for details).

The β-sheets were then generated by duplicating the β_1 and β_2 strands along the direction of the backbone N-H and C=O bonds with PYMOL, using the inter-strand distance of 4.8 Å [36], typical of the parallel register. Eight β-strands for each β_1 and β_2 sheets were generated, considering for the β_2-sheet an interlaced arrangement of the Aβ(1-40) and Aβ(1-42) monomers.

The turn regions were randomly generated using MODELLER [37] and the final one was selected from the resulting pool of 50 structures.

The inter-protofilament structural models were generated by docking calculations starting from two β_2-sheets belonging to two different protofilaments and imposing non-crystallographic symmetry restraints between the two β_2-sheets.

During HADDOCK calculations, first the β_1- and β_2-strands were docked to one another, using all the experimental long-range β_1-β_2 restraints of β_1- and β_2-strands. The lower distance cutoff was set to 3.0 Å, and the upper to 6.0 Å for the shorter mixing times (100 and 200 ms) and to 7.5-8.0 Å for longer mixing (300 and 400 ms). The charges on the N- and C-termini of the β_1-strands and on the N-termini of the β_2-strands were not included in the calculations in order to prevent electrostatic interactions, which do not exist when the two β-strands are linked by a turn region. The histidine protonation states were automatically determined by the Molprobity module embedded in the HADDOCK server. During the rigid docking calculations, 1000 structures were generated, then the best 200 structures were selected for the semi-rigid simulated annealing in torsion angle space, and finally refined in Cartesian space with explicit solvent.

The structural models were then generated by implementing in the calculations all the observed intermolecular β_2-β_2 long-range contacts and inter-strand distance restraints. All the restraints were duplicated symmetrically between the two β_2-sheets using the same protocol used for structural calculations of symmetric protein dimers. Since these long-range distance restraints could be identified only using long mixing times, the upper distance cutoffs in the HADDOCK calculation was set to 8.0 Å. Semi-flexible refinement was enabled on both β_2-sheets.

The family of structures obtained for the mixed Aβ(1-42) and Aβ(1-40) fibrils have been deposited in the protein data bank (model B, PDB ID: 6TI6 and model C, PDB ID:6TI7), together with the structure of the pure Aβ(1-40) fibrils previously reported by Bertini and co-workers (model D, PDB ID: 6TI5, BMRB ID: 34454) [2].

References:

1 F. Ravotti, M. A. Wälti, P. Güntert, R. Riek, A. Böckmann and B. H. Meier, *Biomol. NMR Assign.*, 2016, **10**, 269–276.
2 I. Bertini, L. Gonnelli, C. Luchinat, J. Mao and A. Nesi, *J. Am. Chem. Soc.*, 2011, **133**, 16013–16022.
3 J. T. Nielsen, M. Bjerring, M. D. Jeppesen, R. O. Pedersen, J. M. Pedersen, K. L. Hein, T. Vosegaard, T. Skrydstrup, D. E. Otzen and N. C. Nielsen, *Angew. Chem. Int. Ed Engl.*, 2009, **48**, 2118–2121.
4 S. J. de Vries, M. van Dijk and A. M. J. J. Bonvin, *Nat. Protoc.*, 2010, **5**, 883–897.
5 A. T. Petkova, W.-M. Yau and R. Tycko, *Biochemistry*, 2006, **45**, 498–512.
6 A. K. Paravastu, R. D. Leapman, W.-M. Yau and R. Tycko, *Proc. Natl. Acad. Sci.*, 2008, **105**, 18349–18354.
7 M. Ahmed, J. Davis, D. Aucoin, T. Sato, S. Ahuja, S. Aimoto, J. I. Elliott, W. E. Van Nostrand and S. O. Smith, *Nat. Struct. Mol. Biol.*, 2010, **17**, 561–567.
8 Y. Xiao, B. Ma, D. McElheny, S. Parthasarathy, F. Long, M. Hoshi, R. Nussinov and Y. Ishii, *Nat. Struct. Mol. Biol.*, 2015, **22**, 499–505.
9 M. T. Colvin, R. Silvers, Q. Z. Ni, T. V. Can, I. Sergeyev, M. Rosay, K. J. Donovan, B. Michael, J. Wall, S. Linse and R. G. Griffin, *J. Am. Chem. Soc.*, 2016, **138**, 9663–9674.
10 M. A. Wälti, F. Ravotti, H. Arai, C. G. Glabe, J. S. Wall, A. Böckmann, P. Güntert, B. H. Meier and R. Riek, *Proc. Natl. Acad. Sci. U. S. A.*, 2016, **113**, E4976-4984.
11 K. Rother, P. W. Hildebrand, A. Goede, B. Gruening and R. Preissner, *Nucleic Acids Res.*, 2009, **37**, D393-395.
12 M. T. Colvin, R. Silvers, Q. Z. Ni, T. V. Can, I. V. Sergeyev, M. Rosay, K. J. Donovan, B. Michael, J. S. Wall, S. Linse and R. G. Griffin, *J. Am. Chem. Soc.*, , DOI:10.1021/jacs.6b05129.
13 E. Hellstrand, B. Boland, D. M. Walsh and S. Linse, *ACS Chem. Neurosci.*, 2009, **1**, 13–18.
14 A. Jan, O. Gokce, R. Luthi-Carter and H. A. Lashuel, *J. Biol. Chem.*, 2008, **283**, 28176–28189.
15 D. M. Walsh, D. M. Hartley, Y. Kusumoto, Y. Fezoui, M. M. Condron, A. Lomakin, G. B. Benedek, D. J. Selkoe and D. B. Teplow, *J. Biol. Chem.*, 1999, **274**, 25945–25952.
16 D. M. Walsh, E. Thulin, A. M. Minogue, N. Gustavsson, E. Pang, D. B. Teplow and S. Linse, *FEBS J.*, 2009, **276**, 1266–1281.
17 O. Szczepankiewicz, B. Linse, G. Meisl, E. Thulin, B. Frohm, C. Sala Frigerio, M. T. Colvin, A. C. Jacavone, R. G. Griffin, T. Knowles, D. M. Walsh and S. Linse, *J. Am. Chem. Soc.*, 2015, **137**, 14673–14685.
18 J. Marley, M. Lu and C. Bracken, *J. Biomol. NMR*, 2001, **20**, 71–75.
19 J. R. Brender, A. Ghosh, S. A. Kotler, J. Krishnamoorthy, S. Bera, V. Morris, T. B. Sil, K. Garai, B. Reif, A. Bhunia and A. Ramamoorthy, *Chem. Commun. Camb. Engl.*, 2019, **55**, 4483–4486.
20 B. R. Sahoo, M. E. Bekier, Z. Liu, V. Kocman, A. K. Stoddard, G. M. Anantharamaiah, J. Nowick, C. A. Fierke, Y. Wang and A. Ramamoorthy, *J. Mol. Biol.*, 2020, **432**, 1020–1034.
21 S. Yoo, S. Zhang, A. G. Kreutzer and J. S. Nowick, *Biochemistry*, 2018, **57**, 3861–3866.
22 I. Bertini, F. Engelke, L. Gonnelli, B. Knott, C. Luchinat, D. Osen and E. Ravera, *J. Biomol. NMR*, 2012, **54**, 123–127.
23 A. Böckmann, C. Gardiennet, R. Verel, A. Hunkeler, A. Loquet, G. Pintacuda, L. Emsley, B. H. Meier and A. Lesage, *J. Biomol. NMR*, 2009, **45**, 319–327.
24 A. Schuetz, C. Wasmer, B. Habenstein, R. Verel, J. Greenwald, R. Riek, A. Böckmann and B. H. Meier, *ChemBioChem*, 2010, **11**, 1543–1551.
25 S. Sun, Y. Han, S. Paramasivam, S. Yan, A. E. Siglin, J. C. Williams, I.-J. L. Byeon, J. Ahn, A. M. Gronenborn and T. Polenova, in *Protein NMR Techniques*, eds. A. Shekhtman and D. S. Burz, Humana Press, Totowa, NJ, 2012, pp. 303–331.
26 N. M. Loening, M. Bjerring, N. C. Nielsen and H. Oschkinat, *J. Magn. Reson. San Diego Calif 1997*, 2012, **214**, 81–90.

27 K. Takegoshi, S. Nakamura and T. Terao, *J. Chem. Phys.*, 2003, **118**, 2325–2341.
28 K. Takegoshi, S. Nakamura and T. Terao, *Chem. Phys. Lett.*, 2001, **344**, 631–637.
29 B. Hu, O. Lafon, J. Trébosc, Q. Chen and J.-P. Amoureux, *J. Magn. Reson.*, 2011, **212**, 320–329.
30 W. P. Rothwell and J. S. Waugh, *J. Chem. Phys.*, 1981, **74**, 2721–2732.
31 R. S. Thakur, N. D. Kurur and P. K. Madhu, *Chem. Phys. Lett.*, 2006, **426**, 459–463.
32 R. S. Thakur, N. D. Kurur and P. K. Madhu, *Magn. Reson. Chem. MRC*, 2008, **46**, 166–169.
33 R. S. Thakur, N. D. Kurur and P. K. Madhu, *J. Magn. Reson. San Diego Calif 1997*, 2008, **193**, 77–88.
34 R. Keller, *The Computer Aided Resonance Assignment Tutorial (CARA)*, CANTINA Verlag, Goldau. Switzerland, 2004.
35 Y. Shen, F. Delaglio, G. Cornilescu and A. Bax, *J. Biomol. NMR*, 2009, **44**, 213–223.
36 D. A. Kirschner, C. Abraham and D. J. Selkoe, *Proc. Natl. Acad. Sci. U. S. A.*, 1986, **83**, 503–507.
37 A. Fiser and A. Šali, in *Methods in Enzymology*, ed. Jr. and R. M. S. Charles W. Carter, Academic Press, 2003, vol. Volume 374, pp. 461–491.